JACS
JOURNAL OF THE AMERICAN CHEMICAL SOCIETY

Communication

pubs.acs.org/JACS

Silica Encapsulation of Fluorescent Nanodiamonds for Colloidal Stability and Facile Surface Functionalization

Ambika Bumb,[†,∥] Susanta K. Sarkar,[†,∥] Neil Billington,[‡] Martin W. Brechbiel,[§] and Keir C. Neuman*[,†]

[†]Laboratory of Molecular Biophysics, National Heart, Lung, and Blood Institute, [‡]Cell Biology and Physiology Center, National Heart, Lung, and Blood Institute, and [§]Radiation Oncology Branch, National Cancer Institute, National Institutes of Health, 50 South Drive, Building 50, Room 3517, Bethesda, Maryland 20892, United States

Supporting Information

ABSTRACT: Fluorescent nanodiamonds (FNDs) emit in the near-IR and do not photobleach or photoblink. These properties make FNDs better suited for numerous imaging applications compared with commonly used fluorescence agents such as organic dyes and quantum dots. However, nanodiamonds do not form stable suspensions in aqueous buffer, are prone to aggregation, and are difficult to functionalize. Here we present a method for encapsulating nanodiamonds with silica using an innovative liposome-based encapsulation process that renders the particle surface biocompatible, stable, and readily functionalized through routine linking chemistries. Furthermore, the method selects for a desired particle size and produces a monodisperse agent. We attached biotin to the silica-coated FNDs and tracked the three-dimensional motion of a biotinylated FND tethered by a single DNA molecule with high spatial and temporal resolution.

Fluorescent nanodiamonds (FNDs) are biocompatible nanoparticles with indefinite photostability.[1] Whereas organic dyes photobleach, quantum dots photoblink and raise toxicity concerns, and gold nanoparticles exhibit weak size- and shape-dependent fluorescence, FNDs do not suffer from these nonideal behaviors. Furthermore, their near-IR (NIR) fluorescence (~650 to 900 nm) makes them ideally suited for in vivo imaging.[1] The nitrogen-vacancy centers in these FNDs absorb broadly from 500 to 625 nm and have a peak emission at 690 nm [Figure S2 in the Supporting Information (SI)]. This is beneficial because absorption by blood, water, and proteins in the NIR region is considerably weaker, and thus, NIR light can penetrate tissue to depths of several centimeters.[2,3] Additionally, imaging agents in the NIR region minimize signal contamination from autofluorescence arising from intrinsic fluorophores that typically emit in the visible spectrum.[4,5] The large Stokes shift (>100 nm) of FNDs affords a further reduction in the autofluorescence background. However, biomedical applications of FNDs have faced two challenges due to the inherent properties of the material: (1) aggregation that leads to precipitation and (2) difficulty in functionalizing the inert diamond surface.

Biofunctionalization of FNDs can be achieved by non-covalent adsorption through weak interactions, such as hydrogen bonding, electrostatic forces, $\pi-\pi$ stacking, van der Waals forces, and hydrophobic and hydrophilic interactions.[7] However, more stable and specific bonds are created by covalently linking FNDs to the desired biomolecule. Several methods of introducing functional groups to diamond surfaces have been described.[8] One drawback of some of these techniques is that they require surface modification of the diamond followed by functionalization. This can be an incomplete process and, particularly for the case of detonation diamonds, the precise nature and constituents of the surface may not be well-defined.[9]

Silica coating can assist in maintaining the stability of particle suspensions over a range of pH or electrolyte concentrations as a result of silanol groups that render the surface lyophilic.[10] Silica-coated materials are dispersible in aqueous and nonaqueous solutions, resistant to swelling with changes in solvent polarity, resistant to microbial attack, nontoxic, and biocompatible.[11] Additionally, silica is optically transparent,[12] allowing efficient transmission of excitation and emission light. Finally, the surface silanol groups readily react with alcohols and silane coupling agents,[13] affording covalent bonding with a variety of ligands, including targeting agents such as antibodies and peptides as well as sugars and nucleotides.

To overcome the difficulties of functionalizing FNDs, we have developed a liposome-based encapsulation process to trap them in a silica shell (Figure 1a). This encapsulation renders the FNDs biocompatible, stable, and easily modified through additional conjugation reactions. In addition, the method self-selects for a desired size and produces a monodisperse agent. Coated FNDs exhibit dramatically different properties than uncoated FNDs. Most noted is their improved colloidal stability. Uncoated FNDs rapidly precipitate out of solution (Figure 2a,b), whereas coated FNDs remain in solution for months. Characterization of particle size and surface charge is essential for understanding how to attach particles to surfaces and predicting how an agent will behave in vivo. As shown in Figure 2, uncoated type-1b FNDs have large hydrodynamic diameters (D_H) and low surface charge at pH below 5 (Figure 2c,d). When the surface charge of a particle is low, electrostatic repulsion is not sufficient to prevent the particles from aggregating and flocculating, so D_H and the polydispersity index (PDI), an indicator of aggregation, increase. For uncoated FNDs, the PDI was >0.5 and reached a maximum of 1 at pH below 10, indicating that the FNDs were polydisperse and aggregation had occurred. The coated FNDs, on the other hand, were monodisperse with PDI values below 0.2, particularly at pH above 3, where a strong negative ζ potential (−35 mV)

Received: February 23, 2013
Published: April 12, 2013

dx.doi.org/10.1021/ja4016815 | J. Am. Chem. Soc. 2013, 135, 7815−7818

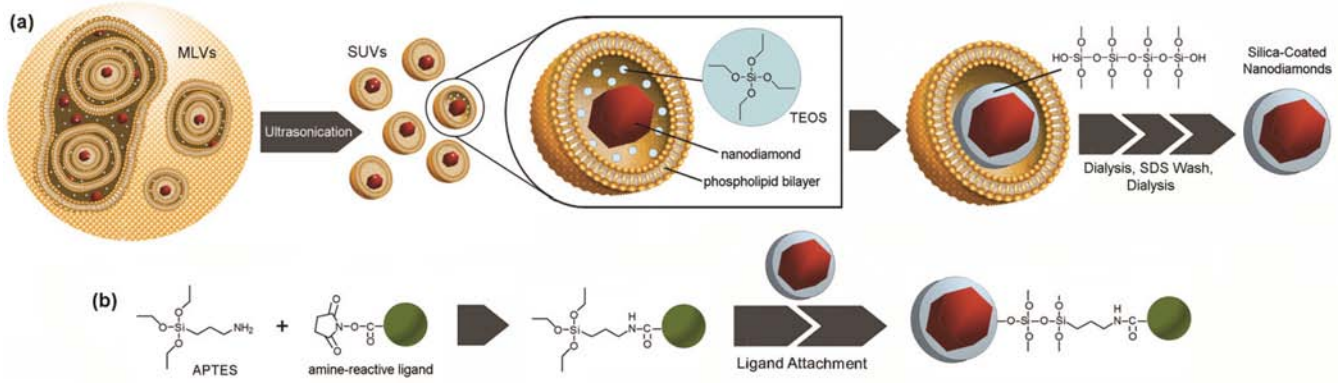

Figure 1. (a) Nanodiamonds in a solution of tetraethyl orthosilicate (TEOS) are trapped in 1-palmitoyl-2-oleoyl-*sn*-glycero-3-phosphocholine (POPC) multilamellar vesicles (MLVs) that can range in size from 500 to 10 000 nm. Ultrasonication breaks the MLVs into small unilamellar vesicles (SUVs) with nominal diameters of ∼100 nm. TEOS is converted into silica, catalyzed by triethylamine (TEA). Thereafter, free TEOS and TEA are dialyzed away. A sodium dodecyl sulfate (SDS) wash breaks up the liposomes to free the coated nanodiamonds, and the remaining reagents (i.e., SDS and POPC) are removed by dialysis. The final product is stabilized and monodisperse silica-encapsulated nanodiamonds. (b) Since the surface of the silica-encapsulated nanodiamonds presents free silanol groups, a variety of silane agents can be used to attach biomolecules to the encapsulated diamonds. One method would be to conjugate a ligand to the amine of APTES and use the remaining silane moieties of APTES to form a linkage with the surface of the particle.

allowed the particles to remain in colloidal suspension with $D_H \approx$ 45 nm. Thus, encapsulating the FNDs with silica made them anionic, stable, and monodisperse across the working pH range (5−8) compared with uncoated FNDs. The coated FNDs' negative charge over the physiological pH range of 6−7 is desirable because it mimics the negative charge of most biomolecules,[14] making them ideal for biomedical applications. Silica coating of the FNDs was confirmed by FTIR analysis (Figure 2e,f), which revealed characteristic silica bands between 800 and 1260 cm^{-1} corresponding to the superimposition of multiple SiO_2 and Si−OH peaks.[6] The strong absorption bands at 1090 and 950 cm^{-1} correspond to the asymmetric vibrations of Si−O and Si−OH, respectively. The same encapsulation process was tested with four different types and sizes of nanodiamonds obtained from various sources. Similar results were found with each, indicating that the method is broadly applicable regardless of the type of nanodiamonds used.

The second reason for encapsulating FNDs with silica was to facilitate the attachment of ligands enabling specific targeting of the FNDs. Silica is easily functionalized using silane coupling agents containing a functional group that can be used for covalent attachment, such as an amine that can react with *N*-hydroxysuccinimide esters or isothiocyanates (Figure 1b). As a proof of principle, an amine-reactive biotin moiety was conjugated to the silica-coated FNDs using 3-aminopropyl-triethoxysilane (APTES) as an intermediate linker. The amine group was reacted with the biotin, and the three ethoxysilyl groups were attached to the silanol groups of the encapsulated FNDs by the Stöber reaction[15] (Figure 1b).

Biotinylation of FNDs was tested at the single-molecule level by using a prism-type total internal reflection fluorescence microscope (TIRFM) (Figure 3a) to quantify the specific binding of the FNDs to a surface passivated with poly(ethylene glycol) (PEG) sparsely labeled with streptavidin (see the SI). On these surfaces, the binding of the biotinylated silica-coated FNDs was ∼15-fold greater than that of the nonbiotinylated silica-coated FNDs (Figure 3). This demonstrates that the coated FNDs were successfully biotinylated and provides additional evidence that the FNDs were encapsulated with silica, which is required for the biotin linking chemistry.

The unique optical properties of FNDs, combined with our robust encapsulation and labeling scheme, make them almost ideal single-molecule tracking probes. We demonstrated this potential by measuring the three-dimensional (3D) motion of a single FND tethered by a DNA molecule with high temporal and spatial resolution over an extended period of time. Tethered particle motion (TPM) of beads attached to DNA or RNA molecules is a robust and sensitive single-molecule method for studying the physical properties of nucleic acids and their interactions with proteins.[16] In contrast to force-based methods such as optical and magnetic tweezers and atomic force microscopy, TPM affords single-molecule measurements of physical properties and interactions in the absence of an applied force. Figure 4 shows the results of 3D TPM measurements on a 1.4 μm DNA molecule with a silica-coated and biotinylated ∼30 nm diameter FND attached to the free end via a biotin−streptavidin linkage. A prism-type TIRFM was used to record the FND fluorescence for ∼1 h with 30 ms time resolution and 20−70 nm spatial resolution (see the SI). Background fluorescence in the field of view was eliminated by photobleaching the observation area prior to tracking the FND, which does not photobleach. In-plane motion (x and y) was tracked with a Gaussian localization tracking routine,[17] whereas out-of-plane motion (z) was tracked by relating the fluorescence intensity to the position of the FND relative to the slide surface; the intensity is proportional to the evanescent excitation field, which decreases exponentially with distance from the surface (see the SI). The probability distributions for the x and y positions are well-described by the Gaussian Random Walk (GRW) model[18,19] (Figure 4e,f). The probability distribution for the z position reflects the restricted motion of the FND due to the surface (Figure 4g) and is well-described by a difference of two Gaussians, which is predicted in the long-chain limit of the GRW.[20] With a contour length (L) of 1.4 μm, fits to the three distributions (Figure 4e−g) returned an average persistence length (l_p) of 55 ± 6 nm, consistent with the accepted DNA persistence length.

Because of the small size of the FND relative to the characteristic length scale of the DNA $[\sim(Ll_p)^{1/2}]$, we expect that the dynamics of the DNA were minimally influenced by the FND. More precisely, the excursion number N_r, defined as N_r =

dx.doi.org/10.1021/ja4016815 | *J. Am. Chem. Soc.* 2013, 135, 7815−7818

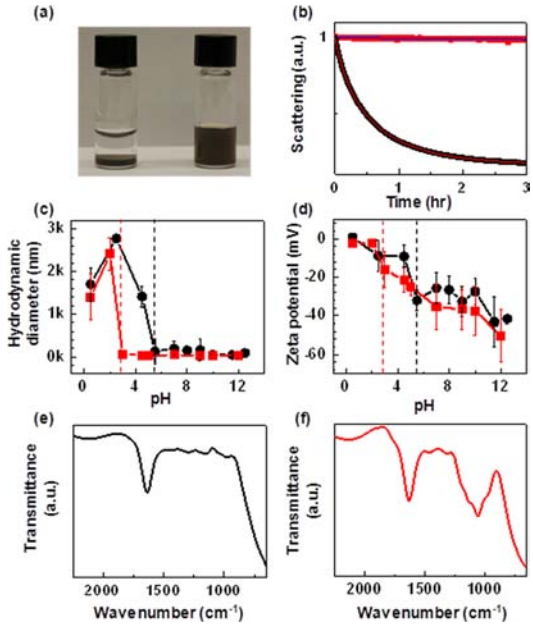

Figure 2. (a) Uncoated (left vial) and silica-coated (right vial) nanodiamonds in water. (b) Settling of uncoated (black symbols) and silica-coated (red symbols) nanodiamonds measured by light scattering. Samples were excited at 635 nm, and the scattering light was measured at 90° relative to the excitation beam. Settling of the coated nanodiamonds was fit to a single exponential with an offset, $I(t) = a_0 + a_1 \exp(-t/t_1)$, with fit parameters $a_0 = 0.9784 \pm 0.0006$ a.u., $a_1 = 0.0220 \pm 0.0005$ a.u., and $t_1 = 4.20 \pm 0.15$ h (blue line), which we interpret as a majority component (98%) that is stable and a minority component (2%) that settles out slowly with a time constant of 4 h. Error bars are the standard error of the fit. Settling of the uncoated nanodiamonds was best fit to a double exponential with an offset, $I(t) = a_0 + a_1 \exp(-t/t_1) + a_2 \exp(-t/t_2)$, with fit parameters $a_0 = 0.1635 \pm 0.0001$ a.u., $a_1 = 0.5534 \pm 0.0010$ a.u., $t_1 = 0.7866 \pm 0.0012$ h, $a_2 = 0.2786 \pm 0.0010$ a.u., and $t_2 = 0.2189 \pm 0.0007$ h (red line). The small values of a_0 and the time constants indicate that the majority (83%) of the uncoated nanodiamonds precipitate in less than 1 h. (c) The hydrodynamic diameter (z average) and (d) ζ potential of silica-coated (red) and uncoated (black) nanodiamonds as a function of pH. At pH below the dotted lines, the absolute value of the ζ potential was <20 mV and flocculation with increased size was observed. Error bars are 1 standard deviation. (e, f) FTIR spectra of (e) uncoated and (f) silica-coated FNDs. Characteristic SiO_2 bands between 800 and 1260 cm^{-1}, the Si−O band at 1090 cm^{-1}, and the Si−OH band at 950 cm^{-1} are apparent in (f). In both FND samples, water was present. The band at 1635 cm^{-1} is due to the scissor bending vibration of molecular water.[6]

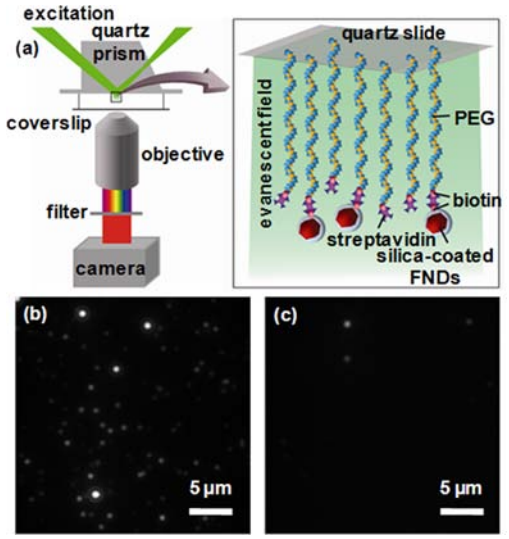

Figure 3. (a) Schematic of single-molecule binding experiment. A quartz slide passivated with biotinylated PEG was saturated with streptavidin. Biotinylated FNDs were flowed into the flow cell, and specific attachment to streptavidin−biotin-PEG was probed by comparing the number of bound particles before and after washing to remove nonspecifically bound particles. FNDs were excited by the evanescent field (green) in a prism-type TIRFM (see the SI). (b, c) Images showing that (b) 60% of the biotinylated silica-coated FNDs and (c) 4% of the nonbiotinylated silica-coated FNDs remained attached to the surface after the stringent acid−base wash (Figure S1 shows the before-wash images).

$r(Ll_p/3)^{-1/2}$, where r is the radius of the FND, provides a measure of the influence of the FND on the dynamics of the polymer tether.[19] For $N_r < 1$, the dynamics are dominated by the DNA tether, whereas for increasing values of $N_r \geq 1$, the FND increasingly influences the motion.[19] For the silica-coated ~30 nm diameter FND and the 1.4 μm DNA tether, $N_r = 0.09$. Indeed, for 30 nm diameter FNDs, $N_r = 1$ for $L \approx 14$ nm (~40 base pairs), assuming $l_p \approx 50$ nm. Therefore, FNDs provide a suitable tracking probe for studying the dynamics of polymers such as DNA with short contour lengths. Along with being minimally perturbative, TPM tracking of FNDs in the evanescent field affords low background while providing a sensitive measure of z motion (Figure 4). Tracking of z motion is difficult in traditional bead-based TPM measurements but has been achieved with specialized evanescent dark-field scattering measurements with colloidal gold particles.[18] TPM measurements using FNDs share the advantages of small radius, high temporal and spatial resolution, long-term photostability, and straightforward tracking of z motion afforded by laser scattering from gold nanoparticles but can be performed on a standard TIRFM and do not suffer from the technical challenges associated with detecting weak scattered light.[18] These measurements demonstrate that functionalized FNDs can be used as sensitive and photostable probes for tracking the 3D motion of biomolecules with high spatial and temporal resolution.

In summary, we have presented a simple and robust method for encapsulating nanodiamonds with silica. The encapsulation process can be readily used to stabilize and functionalize any nanodiamond with a thin silica shell independent of its surface properties. Once encapsulated with silica, the nanodiamonds are readily further modified through established silica functionalization schemes. We have demonstrated the utility of this approach by covalently attaching biotin to FNDs and tracking the 3D motion of a single biotinylated FND attached to an individual DNA molecule with high spatial and temporal resolution over an extended period of time. Optically superior, stable, and functionalizable FNDs have a plethora of applications in the fields of nanotechnology and nanomedicine. For instance, silica-coated FNDs can be functionalized for multimodal imaging with radiolabels and magnetic resonance imaging contrast agents for targeted drug delivery with tracking ability. At the single-molecule level, they can be used to track labeled biomolecules over extended periods of time, and because of their wide excitation spectra, they can be used as stable fiducial markers for ultrahigh-resolution microscopy across multiple wavelengths. The energy level structure and electron spin coherence of FNDs also facilitates applications in ultralow magnetic field detection and ultrasensitive NMR spectroscopy.[21] Therefore, the ability to

dx.doi.org/10.1021/ja4016815 | J. Am. Chem. Soc. 2013, 135, 7815−7818

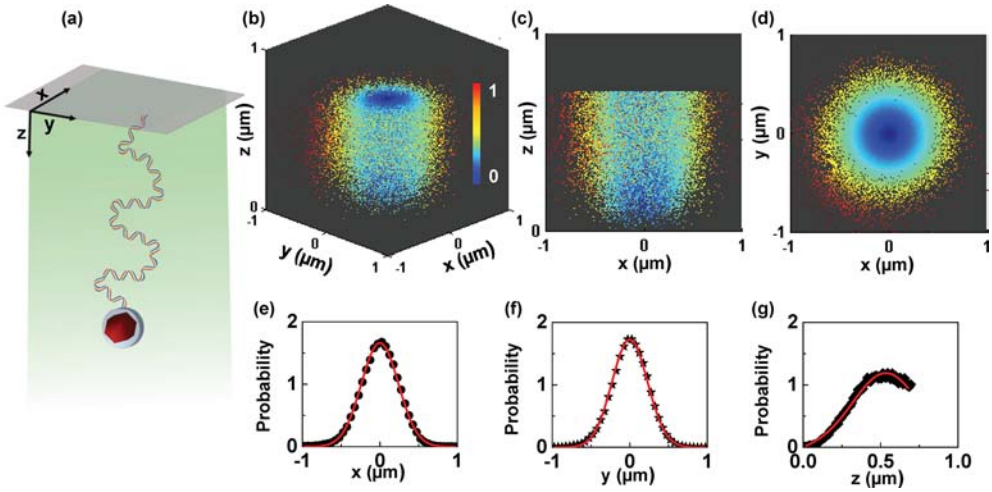

Figure 4. 3D TPM measurements of DNA conformations using biotinylated FNDs. (a) One end of a 1.4 μm double-stranded DNA molecule was tethered to a quartz slide and the other end to a biotinylated ~30 nm FND. The FND was excited by the evanescent wave created at the interface of the quartz slide and the buffer in the flow cell in a prism-type TIRFM. The evanescent field (green) decreases exponentially with the distance from the quartz−buffer interface. Custom tracking software was used to track the x and y positions and the intensity (I) of the FND; ln I provides a measure of the z position as the FND moves in the exponentially varying evanescent field. An intensity threshold was used to avoid tracking errors, which resulted in missing positions of the FND at large z extension, leading to the flat tops in the distributions in (b) and (c). (b) Front, (c) side, and (d) top views of a scatter plot of the x, y, and z coordinates of the tethered FND (n = 54 263), where z = 0 denotes the position of maximum intensity, assumed to be the quartz−buffer interface. Points are color-coded according to $r^2 = x^2 + y^2$, with r = 0 shown in blue and r = 1 in red. (e−g) Area-normalized probability densities along x, y, and z, respectively (see the SI). The DNA persistence length obtained from fits to the distributions is 55 ± 6 nm (mean ± standard deviation). The cutoff in (g) corresponds to the intensity threshold used in the tracking software.

silica-coat and functionalize FNDs provides a unique nanomaterial for wide range of biological imaging applications.

■ ASSOCIATED CONTENT

Supporting Information

Additional figures, equations for Figure 4e−g, and experimental details. This material is available free of charge via the Internet at http://pubs.acs.org.

■ AUTHOR INFORMATION

Corresponding Author

neumankc@mail.nih.gov

Author Contributions

‖A.B. and S.K.S. contributed equally.

Notes

The authors declare no competing financial interest.

■ ACKNOWLEDGMENTS

This research was supported by the National Institutes of Health (NCI and NHLBI). We thank Joe Barchi for help with FTIR, the NHLBI Biophysical Core Facility and Grzegorz Piszczek for help with scattering measurements, Jonathan Silver for help in preparing the DNA molecules, Richard Leapman and Maria Aronova at NIBIB for assistance, and Gopalakrishnan Balasubramanian for helpful discussions.

■ REFERENCES

(1) Yu, S.-J.; Kang, M.-W.; Chang, H.-C.; Chen, K.-M.; Yu, Y.-C. *J. Am. Chem. Soc.* **2005**, *127*, 17604.

(2) Bumb, A.; Regino, C.; Perkins, M.; Bernardo, M.; Ogawa, M.; Fugger, L.; Choyke, P.; Dobson, P.; Brechbiel, M. *Nanotechnology* **2010**, *21*, No. 175704.

(3) Grosenick, D.; Wabnitz, H.; Rinneberg, H. H.; Moesta, K. T.; Schlag, P. M. *Appl. Opt.* **1999**, *38*, 2927.

(4) Andersson-Engels, S.; Wilson, B. C. *J. Cell Pharmacol.* **1992**, *3*, 48.

(5) Weissleder, R. *Nat. Biotechnol.* **2001**, *19*, 316.

(6) Beganskienė, A.; Sirutkaitis, V.; Kurtinaitiene, M.; Juškėnas, R.; Kareiva, A. *Mater. Sci.* **2004**, *10*, 287.

(7) Xing, Y.; Dai, L. *Nanomedicine* **2009**, *4*, 207.

(8) Mochalin, V. N.; Shenderova, O.; Ho, D.; Gogotsi, Y. *Nat. Nanotechnol.* **2012**, *7*, 11.

(9) Kuznetsov, O.; Sun, Y.; Thaner, R.; Bratt, A.; Shenoy, V.; Wong, M. S.; Jones, J.; Billups, W. *Langmuir* **2012**, *28*, 5243.

(10) Mulvaney, P.; Liz-Marzán, L.; Giersig, M.; Ung, T. *J. Mater. Chem.* **2000**, *10*, 1259.

(11) (a) Jin, Y.; Kannan, S.; Wu, M.; Zhao, J. X. *Chem. Res. Toxicol.* **2007**, *20*, 1126. (b) Xue, Z.; Liang, D.; Li, Y.; Long, Z.; Pan, Q.; Liu, X.; Wu, L.; Zhu, S.; Cai, F.; Dai, H. *Chin. Sci. Bull.* **2005**, *50*, 2323.

(12) Liu, D. M.; Chen, I. *Acta Mater.* **1999**, *47*, 4535.

(13) Ulman, A. *Chem. Rev.* **1996**, *96*, 1533.

(14) Vroman, L. *Science* **1974**, *184*, 585.

(15) Stöber, W.; Fink, A.; Bohn, E. *J. Colloid Interface Sci.* **1968**, *26*, 62.

(16) (a) Dunlap, D.; Zurla, C.; Manzo, C.; Finzi, L. *Methods Mol. Biol.* **2011**, *783*, 295. (b) Schafer, D. A.; Gelles, J.; Sheetz, M. P.; Landick, R. *Nature* **1991**, *352*, 444.

(17) Sarkar, S. K.; Marmer, B.; Goldberg, G.; Neuman, K. C. *Curr. Biol.* **2012**, *22*, 1047.

(18) Lindner, M.; Nir, G.; Medalion, S.; Dietrich, H. R. C.; Rabin, Y.; Garini, Y. *Phys. Rev. E* **2011**, *83*, No. 011916.

(19) Segall, D. E.; Nelson, P. C.; Phillips, R. *Phys. Rev. Lett.* **2006**, *96*, No. 088306.

(20) Blumberg, S.; Gajraj, A.; Pennington, M. W.; Meiners, J. C. *Biophys. J.* **2005**, *89*, 1272.

(21) (a) Balasubramanian, G.; Chan, I. Y.; Kolesov, R.; Al-Hmoud, M.; Tisler, J.; Shin, C.; Kim, C.; Wojcik, A.; Hemmer, P. R.; Krueger, A.; Hanke, T.; Leitenstorfer, A.; Bratschitsch, R.; Jelezko, F.; Wrachtrup, J. *Nature* **2008**, *455*, 648. (b) Epstein, R.; Mendoza, F.; Kato, Y.; Awschalom, D. *Nat. Phys.* **2005**, *1*, 94. (c) Takahashi, S.; Hanson, R.; van Tol, J.; Sherwin, M. S.; Awschalom, D. D. *Phys. Rev. Lett.* **2008**, *101*, No. 047601.